CHAPTER 7 Making Waves

7.1 The shallow-water equations

In most of this chapter we will discuss the shallow-water equations, which can be written as

$$\frac{\partial \mathbf{v}}{\partial t} + (\zeta + f)\hat{\mathbf{k}} \times \mathbf{v} = -\nabla[g(h + h_s) + K] \tag{7.1}$$

$$\frac{\partial h}{\partial t} + \nabla \bullet (\mathbf{v}h) = 0 . \tag{7.2}$$

Here $\mathbf{v}$ is the horizontal velocity vector, $\zeta \equiv \mathbf{k} \bullet (\nabla \times \mathbf{v})$ is the vertical component of the vorticity, f is the coriolis parameter, h is the depth of the fluid, h_s is the height of the "bottom topography," g is the acceleration of gravity, and $K \equiv \frac{1}{2}\mathbf{v} \bullet \mathbf{v}$ is the kinetic energy per unit mass. In (7.1), all frictional effects have been neglected, for simplicity.

A very useful idealized subset of the shallow-water system describes the special case of a one-dimensional, small-amplitude, external gravity wave for a shallow, non-rotating incompressible, homogeneous fluid (shallow water), with a resting basic state. Eqs. (7.1) and (7.2) become

$$\frac{\partial u}{\partial t} + g\frac{\partial h}{\partial x} = 0 , \tag{7.3}$$

and

$$\frac{\partial h}{\partial t} + H\frac{\partial u}{\partial x} = 0 , \tag{7.4}$$

respectively. Here H is the mean depth of the fluid. We refer to (7.3)-(7.4) as “the gravity wave equations.” Let

$$c^2 \equiv gH\,. \tag{7.5}$$

By combining (7.3)-(7.4) we can derive

$$\frac{\partial^2 u}{\partial t^2} = c^2 \frac{\partial^2 u}{\partial x^2} \tag{7.6}$$

and

$$\frac{\partial^2 h}{\partial t^2} = c^2 \frac{\partial^2 h}{\partial x^2}\,, \tag{7.7}$$

which are both examples of "the wave equation."

Assuming solutions of the form $e^{i(kx-\omega t)}$, we obtain the dispersion equation

$$\omega^2 = gHk^2 \tag{7.8}$$

The exact phase speed of pure gravity waves (without the effects of rotation) is $\pm\sqrt{gH}$, regardless of wave length. There are two waves, one propagating in the positive x-direction, and the other in the negative x-direction.

7.2 The wave equation

The solutions of the wave equation, (7.6), are constant along space-time line (or surfaces) called "characteristics." A solution is fully determined if u and $\frac{\partial u}{\partial t}$ are specified somewhere on each characteristic. The characteristics can, and generally do, intersect boundaries. As with the advection equation, $f(x-ct)$ is a particular solution of the wave equation (7.6), but $g(x+ct)$ is a second particular solution. We can assume $c>0$ without loss of generality. The general solution of (7.6) is given by

$$u(x,t) = f(x-ct) + g(x+ct)\,, \tag{7.9}$$

where, as shown below, the forms of f and g are determined completely by the initial conditions

$$\begin{aligned} u_{t=0} &= F(x)\,, \\ \left(\frac{\partial u}{\partial t}\right)_{t=0} &= G(x)\,. \end{aligned} \tag{7.10}$$

Substituting (7.9) into (7.10), we find that

$$f(x) + g(x) = F(x) ,$$

$$-cf'(x) + cg'(x) = G(x) . \tag{7.11}$$

Here a prime denotes differentiation. Differentiating the first of (7.11) and then using the second of (7.11), we find that

$$f'(x) = \frac{1}{2}\left[F'(x) - \frac{G(x)}{c}\right] ,$$

$$g'(x) = \frac{1}{2}\left[F'(x) + \frac{G(x)}{c}\right] . \tag{7.12}$$

Integration of (7.12) gives

$$f(x) = \frac{1}{2}\left[F(x) - \frac{1}{c}\int_0^x G(\xi)d\xi\right] + C_1 ,$$

$$g(x) = \frac{1}{2}\left[F(x) + \frac{1}{c}\int_0^x G(\xi)d\xi\right] + C_2 . \tag{7.13}$$

Here C_1 and C_2 are constants of integration. Finally, we obtain $u(x, t)$ by replacing x by $x - ct$ and $x + ct$, respectively, in f and g of (7.13), and then substituting into (7.9). This gives

$$u(x, t) = \frac{1}{2}\left[F(x - ct) + F(x + ct) + \frac{1}{c}\int_{x-ct}^{x+ct} G(\xi)d\xi\right] , \tag{7.14}$$

where we have required and used $C_1 + C_2 = 0$ in order to satisfy $u_{t=0} = F(x)$.

In order to further relate the wave equation to the advection equation that we have already studied, we reduce (7.6) to a pair of first-order equations by defining

$$p \equiv \frac{\partial u}{\partial t} \text{ and } q \equiv -c\frac{\partial u}{\partial x} . \tag{7.15}$$

Substitution of (7.15) into the wave equation (7.6) gives

$$\frac{\partial p}{\partial t} + c\frac{\partial q}{\partial x} = 0 , \tag{7.16}$$

and differentiation of the second of (7.15) with respect to t, with the use of the first of (7.15), gives

$$\frac{\partial q}{\partial t} + c\frac{\partial p}{\partial x} = 0 . \tag{7.17}$$

If we alternately add (7.16) and (7.17) and subtract (7.17) from (7.16), we obtain

$$\frac{\partial P}{\partial t} + c\frac{\partial P}{\partial x} = 0 , \text{ where } P \equiv p + q , \tag{7.18}$$

$$\frac{\partial Q}{\partial t} - c\frac{\partial Q}{\partial x} = 0 , \text{ where } Q \equiv p - q . \tag{7.19}$$

Now we have a system of two first-order equations, each in the form of the advection equation. Note, however, that the "advections" are in opposite directions! Assuming that $c > 0$, P is "advected" towards increasing x, while Q is "advected" towards decreasing x. From (7.18) and (7.19), it is clear that P is constant along the line $x - ct = \text{constant}$, and Q is constant along the line $x + ct = \text{constant}$. Equations (7.18) and (7.19) are called the *normal form* of (7.16) and (7.17).

These concepts are applicable, with minor adjustments, to any hyperbolic system of equations. The curves $x - ct = \text{constant}$ and $x + ct = \text{constant}$ are called "characteristics." A hyperbolic equation is characterized, so to speak, by two such families of curves. In the present case they are straight lines, but in general they can have any shape.

7.3 Staggered grids

Now we discuss the differential-difference equations

$$\frac{\partial u_j}{\partial t} + g\left(\frac{h_{j+1} - h_{j-1}}{2\Delta x}\right) = 0 , \tag{7.20}$$

$$\frac{\partial h_j}{\partial t} + H\left(\frac{u_{j+1} - u_{j-1}}{2\Delta x}\right) = 0 , \tag{7.21}$$

which are, of course, differential-difference analogs of the one-dimensional shallow water equations, (7.3) and (7.4). Consider a distribution of the dependent variables on the grid as shown in Fig. 7.1. Notice that from (7.20) and (7.21) *the set of red quantities will act completely independently of the set of black quantities*, if there are no boundaries. With cyclic

boundary conditions, this is still true if the number of grid points in the cyclic domain is even.

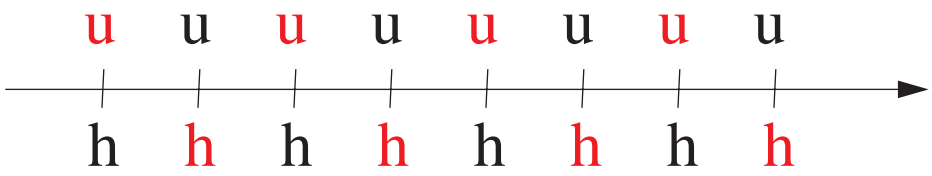

Figure 7.1: A grid for solution of the one-dimensional shallow water equations.

What this means is that we have two families of waves on the grid: "red" waves that propagate both left and right, and "black" waves that propagate both left and right. Physically there should only be one family of waves.

Here is a mathematical way to draw the same conclusion. The wave solutions of (7.20) and (7.21) are

$$(u_j, h_j) \propto e^{i(kj\Delta x - \omega t)} , \tag{7.22}$$

giving

$$\begin{aligned} \omega u_j - g h_j \frac{\sin(k\Delta x)}{\Delta x} &= 0 , \\ \omega h_j - H u_j \frac{\sin(k\Delta x)}{\Delta x} &= 0 . \end{aligned} \tag{7.23}$$

Provided that u_j and h_j are not both identically zero, we obtain the dispersion relation

$$\omega^2 = k^2 g H \left(\frac{\sin p}{p}\right)^2 \text{ where } p \equiv k\Delta x . \tag{7.24}$$

Suppose that ω is given. If $p = p_0$ satisfies (7.24), then $p = -p_0$, $p = \pi - p_0$ and $p = -(\pi - p_0)$ also satisfy it. This shows that there are four possible modes for the given ω, although physically there should only be two. The "extra" pair of modes come from the redundancy on the grid. *The extra modes are computational modes "in space."* Earlier we encountered computational modes in time.

Without loss of generality, we suppose that $0 < p_0 < \frac{\pi}{2}$, so that $\sin(p_0) > 0$. Then the two solutions $p = p_0$ and $p = -p_0$ are approximations to the true solution, and therefore could be considered as "physical," while the other two, $p = \pi - p_0$ and $p = -(\pi - p_0)$, could be considered as "computational." This distinction is less significant than in the case of

the advection equation, however. In the case of advection, the envelope of a computational mode propagates in the downstream direction. In the case of the wave equation, there is no "downstream" direction.

For a given ω, the general solution for u_j is a linear combination of the four modes, and can be written as

$$u_j = [Ae^{ip_0 j} + Be^{-ip_0 j} + Ce^{i(\pi - p_0)j} + De^{-i(\pi - p_0)j}]e^{-i\omega t} . \tag{7.25}$$

Correspondingly, by substituting (7.25) into (7.21), we find that h_j satisfies

$$h_j = \frac{H \sin p_0}{\omega \Delta x}[Ae^{ip_0 j} - Be^{-ip_0 j} + Ce^{i(\pi - p_0)j} - De^{-i(\pi - p_0)j}]e^{-i\omega t} . \tag{7.26}$$

If we assume $\omega > 0$, so that $\sin(p_0) = \frac{\omega \Delta x}{\sqrt{gH}}$ [see (7.24)], then (7.26) reduces to

$$h_j = \sqrt{\frac{H}{g}}[Ae^{ip_0 j} - Be^{-ip_0 j} + Ce^{i(\pi - p_0)j} - De^{i(\pi - p_0)j}]e^{-i\omega t} . \tag{7.27}$$

7.4 Numerical simulation of geostrophic adjustment. as a guide to grid design

Winninghoff (1968) and Arakawa and Lamb (1977; hereafter AL) discussed the extent to which finite-difference approximations to the shallow water equations can simulate the process of geostrophic adjustment, in which the dispersion of inertia-gravity waves leads to the establishment of a geostrophic balance, as the energy density of the inertia gravity waves decreases with time due to their dispersive phase speeds and non-zero group velocity. These authors considered the momentum and mass conservation equations, and defined five different staggered grids for the velocity components and mass.

AL considered the shallow water equations linearized about a resting basic state, in the following form:

$$\frac{\partial u}{\partial t} - fv + g\frac{\partial h}{\partial x} = 0 , \tag{7.28}$$

$$\frac{\partial v}{\partial t} + fu + g\frac{\partial h}{\partial y} = 0 , \tag{7.29}$$

$$\frac{\partial h}{\partial t} + H\delta = 0 . \tag{7.30}$$

Here H is the constant depth of the "water" in the basic state, $\delta \equiv \frac{\partial u}{\partial x} + \frac{\partial v}{\partial y}$ is the divergence,

and all other symbols have their conventional meanings. From (7.28)- (7.30), we can derive an equivalent set in terms of vorticity, $\zeta = \frac{\partial v}{\partial x} - \frac{\partial u}{\partial y}$, and divergence:

$$\frac{\partial \delta}{\partial t} - f\zeta + g\left(\frac{\partial^2}{\partial x^2}h + \frac{\partial^2}{\partial y^2}h\right) = 0 , \tag{7.31}$$

$$\frac{\partial \zeta}{\partial t} + f\delta = 0 , \tag{7.32}$$

$$\frac{\partial h}{\partial t} + H\delta = 0 . \tag{7.33}$$

Of course, (7.33) is identical to (7.30). We can eliminate the vorticity and mass in (7.31) by using (7.32) and (7.33), respectively. Then by assuming wave solutions, we obtain the dispersion relation:

$$\left(\frac{\sigma}{f}\right)^2 = 1 + \lambda^2(k^2 + l^2) . \tag{7.34}$$

Here σ is the frequency, $\lambda \equiv \sqrt{gH}/f$ is the radius of deformation, and k and l are the wave numbers in the x and y directions, respectively. The frequency and group speed increase monotonically with wave number and are non-zero for all wave numbers. As discussed by AL, these characteristics of (7.34) are important for the geostrophic adjustment process.

In their discussion of various numerical representations of (7.28)- (7.30), AL defined five grids denoted by "A" through "E," as shown in Fig. 7.2. Fig. 7.2 also shows the *Z* grid, which will be discussed later. AL also gave the simplest centered finite-difference approximations to (7.28)- (7.30), for each of the five grids; these equations will not be repeated here. The two-dimensional dispersion equations for the various schemes were derived but not published by AL; they are included in Fig. 7.2. The table also gives a plot of the nondimensional frequency, (σ/f), as a function of kd and ld, for the special case $\lambda/d = 2$. Here d is the grid size, assumed to be the same in the x and y directions. The significance of this particular choice of λ/d is discussed later. The plots show how the nondimensional frequency varies out to $kd = \pi$ and $ld = \pi$; these wave numbers correspond to the shortest waves that can be represented on the grid.

The A grid may appear to be the simplest, since it is unstaggered. For example, the coriolis terms of the momentum equations are easily evaluated, since u and v are defined at the same points. Approximation of the spatial derivatives in (1-3) inevitably involves averaging on the A grid, however. To illustrate this important point, consider the simplest centered approximation to $\partial h/\partial x$ at a u point, on the A grid. We must first obtain a value of h at $i + 1/2$ by averaging from i and $i + 1$, and a second value at $i - 1/2$ by averaging from i and $i - 1$. We can then subtract these two average values of h, and divide by Δx, to

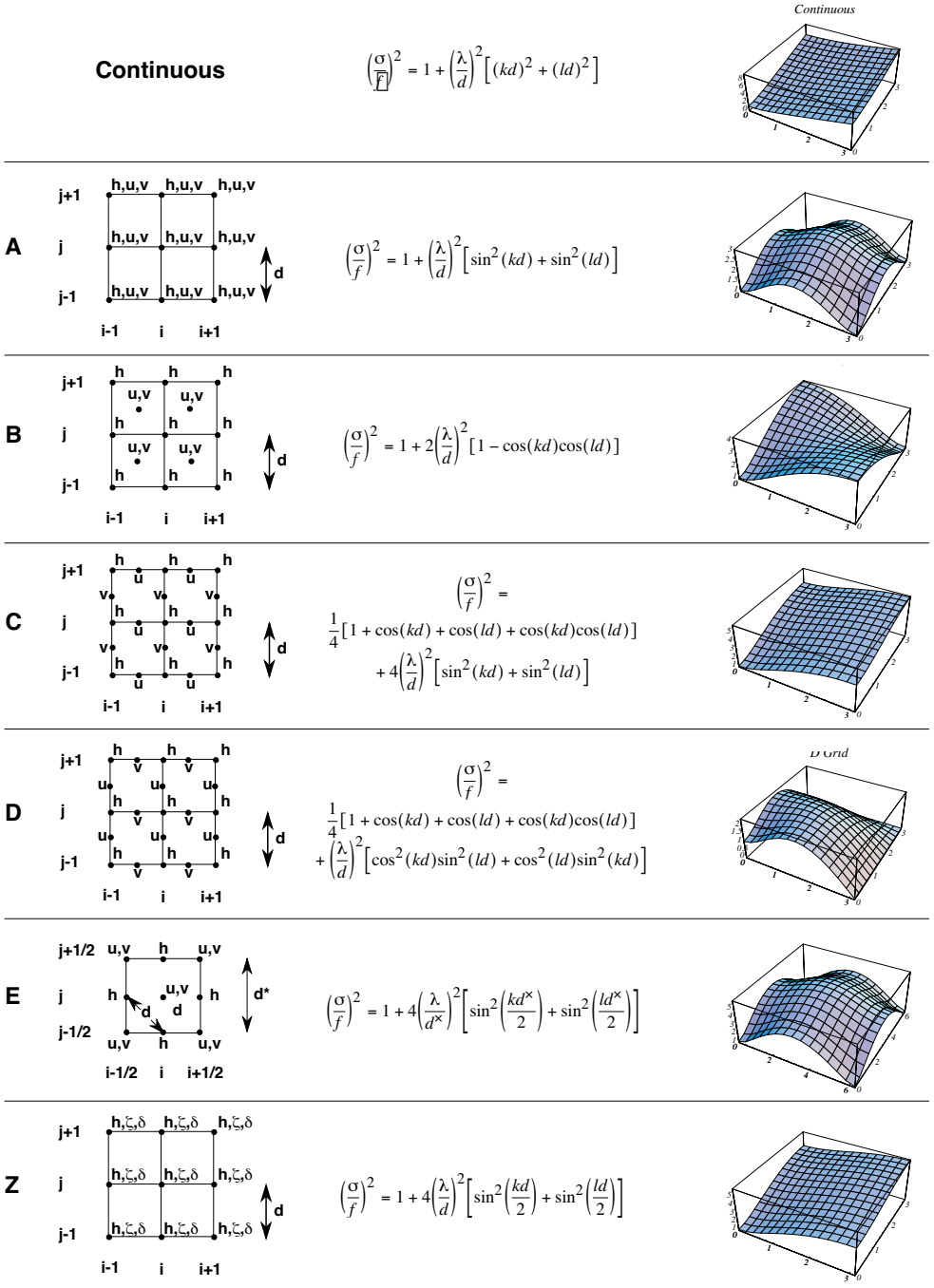

Figure 7.2: **Grids, dispersion equations, and plots of dispersion equations for grids A–E and Z. The continuous dispersion equation and its plot are also shown for comparison. For plotting, it has been assumed that $\lambda/d = 2$.**

obtain the desired approximation to $\partial h/\partial x$. Similarly, averaging is needed to define the mass convergence / divergence at h points.

The averaging described above inevitably "hides" noise at the smallest represented scales (e.g. a checkerboard pattern in h). Such dynamically "invisible" noise cannot participate in the dynamics of the model, e.g. by propagating and dispersing as in the process of geostrophic adjustment. A plot of the dispersion equation for the A grid, as shown in Fig. 7.2, indicates a maximum of the frequency (group speed equal to zero) for some combinations k and l. As a result, solutions on the A grid are extremely noisy in practice and must be smoothed, e.g. through filtering (e.g., Kalnay-Rivas et al., 1977). Because of this well known problem, the A grid is almost never used today.

The preceding discussion is an example which illustrates the general rule that it is desirable to avoid averaging in the design of a finite-difference scheme.

Next, consider the B grid. As on the A grid, the coriolis terms are easily evaluated, without averaging, since u and v are defined at the same points. On the other hand, the pressure-gradient terms must be averaged, again as on the A grid. There is an important difference, however. On the A grid, the averaging used to approximate the x-component of the pressure-gradient force, $\partial h/\partial x$, is averaging *in the x-direction*. On the B grid, the corresponding averages are *in the y-direction*. On the B grid, an oscillation in the x-direction, on the smallest represented scale, is not averaged out in the computation of $\partial h/\partial x$; it can, therefore, participate in the model's dynamics, and so is subject to geostrophic adjustment. A similar conclusion holds for the convergence / divergence terms of the continuity equation. For example, the averaging in the y-direction does no harm for solutions that are uniform in the y-direction. Nevertheless, it does do some harm, as is apparent in the plot of the B-grid dispersion equation, as shown in Fig. 7.2. The frequency does not increase monotonically with total wave number; for certain combinations of k and l, the group speed is zero. AL concluded that the B grid gives a fairly good simulation of geostrophic adjustment, but with some tendency to small-scale noise.

Now consider the C grid. The pressure gradient terms are easily evaluated, without averaging, because h is defined east and west of u points, and north and south of v points. Similarly, the mass convergence / divergence terms of the continuity equation can be evaluated without averaging the winds. On the other hand, averaging *is* needed to obtain the coriolis terms, since u and v are defined at different points. For very small-scale inertia-gravity waves, the coriolis terms are negligible; we essentially have pure gravity waves. This suggests that the C grid will perform well if the horizontal resolution of the model is high enough so that the smallest waves that can be represented on the grid are insensitive to the coriolis force. More precisely, AL argued that the C grid does well when the grid size is small compared to λ, the radius of deformation. A plot of the dispersion equation, given in Fig. 7.2, shows that the frequency increases monotonically with wave number, as in the exact solution, although not as rapidly. Recall, however, that this plot is for the special case $\lambda/d = 2$. We return to this point later.

Next, we turn to the D grid. Inspection of the stencil shown in Fig. 7.2 shows that the D grid allows a simple evaluation of the geostrophic wind. In view of the importance of geostrophic balance for large-scale motions, this may appear to be an attractive property. It is also apparent, however, that considerable averaging is needed in the pressure-gradient force,

mass convergence / divergence, and even in the coriolis terms. As a result, the dispersion equation for the D grid is very badly behaved, giving zero phase speed for the shortest represented waves, and also giving a zero group speed for some modes.

Finally, the E grid is shown in Fig. 7.2. The grid spacing for the E grid is chosen to be $d^* \equiv \sqrt{2}d$, so that the "density" of h points is the same as in the other four grids. The E grid at first seems perfect; no averaging is needed for the coriolis terms, the pressure-gradient terms, or the mass convergence / divergence terms. Nevertheless there is a problem, which becomes apparent if we consider a solution that is uniform in one of the grid directions, say the y-direction. In that case, we effectively have a one-dimensional problem. In one dimension, the E grid "collapses" to the A grid, with a reduced grid spacing $d = d^*/\sqrt{2}$. For such one-dimensional motions, the E grid has all the problems of the A grid. These problems are apparent in the plot of the dispersion equation, given in Fig. 7.2. (For the E grid, the nondimensional frequency is plotted as a function of kd^* and ld^*, out to a value of 2π; this corresponds to the shortest "one-dimensional" mode.) The group speed is zero for some combinations of k and l.

Now recall the conclusion of AL, described earlier, that the C grid gives a good simulation of geostrophic adjustment provided that $\lambda/d > 1$. Large-scale modelers are never happy to choose d so that λ/d can be less than one. Nevertheless, in practice modes for which $\lambda/d \ll 1$ can be unavoidable, at least for some situations. For example, Hansen et al. (1983) described a low-resolution atmospheric GCM, which they called Model II, designed for very long climate simulations in which low resolution was a necessity. Model II used a grid size of 10 degrees of longitude by 8 degrees of latitude; this means that the grid size was larger than the radius of deformation for many of the physically important modes that could be represented on the grid. As shown by AL, such modes cannot be well simulated using the C grid. Having experienced these problems with the C grid, Hansen et al. (1983) chose the B grid for Model II.

Ocean models must contend with small radii of deformation, so that very fine grids are needed to ensure that $\lambda/d > 1$, even for external modes. For this reason, ocean models tend to use the B grid (e.g., Semtner and Chervin, 1992).

In addition, three-dimensional models of the atmosphere and ocean generate internal modes. With vertical structures typical of current general circulation models, the highest internal modes can have radii of deformation on the order of 50 km or less. The same model may have a horizontal grid spacing on the order of 500 km, so that λ/d can be on the order of 0.1. Fig. 7.3 demonstrates that the C grid behaves very badly for $\lambda/d = 0.1$. The phase speed actually decreases monotonically as the wave number increases, and becomes very small for the shortest waves that can be represented on the grid. Janjic and Mesinger (1989) have emphasized that, a result, models that use the C grid have difficulty in representing the geostrophic adjustment of high internal modes. In contrast, the dispersion relation for the B grid is qualitatively insensitive to the value of λ/d. The B grid has moderate problems for $\lambda/d = 2$, but these problems do not become significantly worse for $\lambda/d = 0.1$.

In summary, the C grid does well with deep, external modes, but has serious problems with high internal modes, whereas the B grid has moderate problems with all modes.

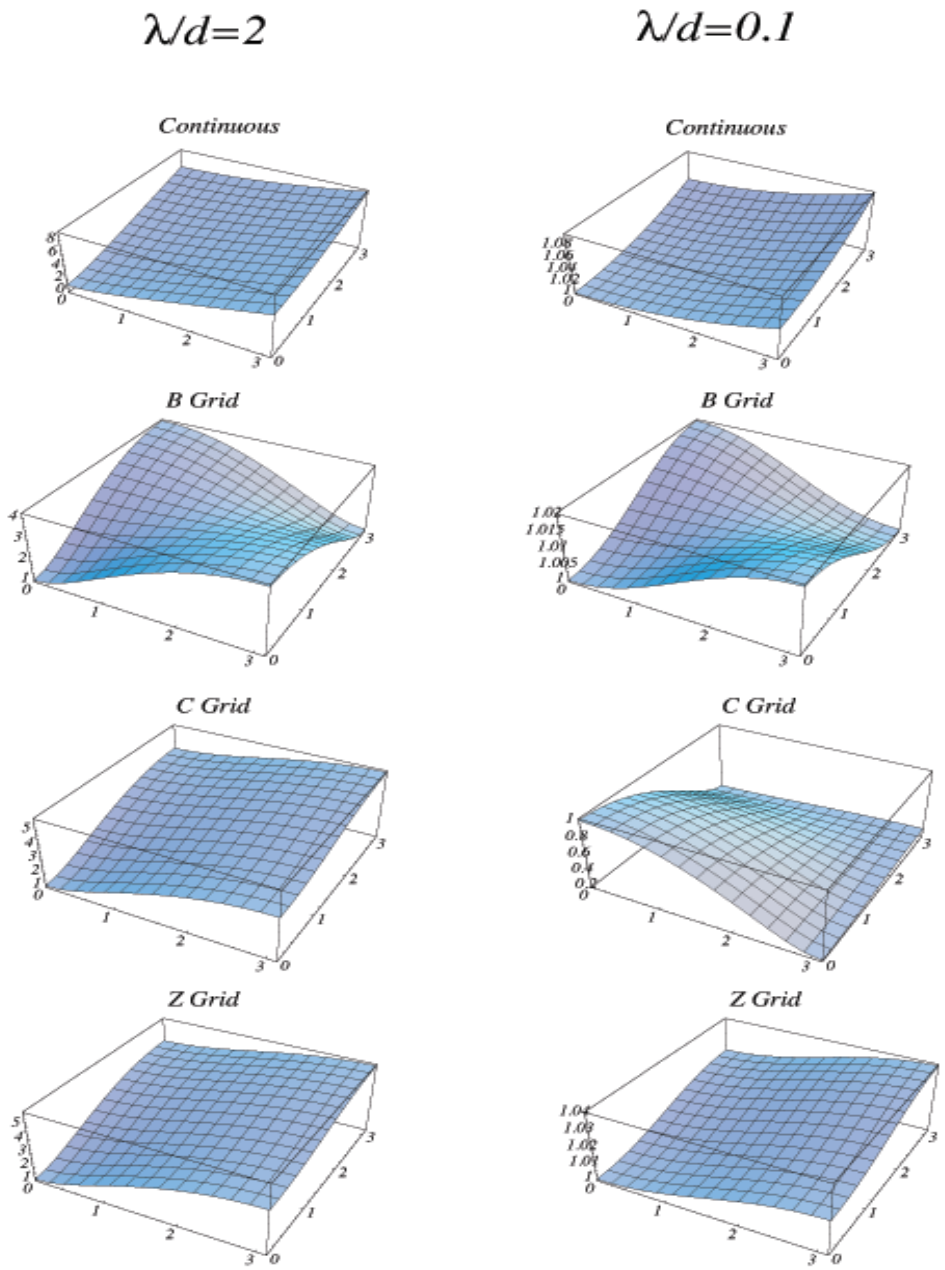

Figure 7.3: Dispersion relations for the continuous shallow water equations, and for finite-difference approximations based on the B, C, and Z grids. The horizontal coordinates in the plots are kd and ld, respectively, except for the E grid, for which kd^* and ld^* are used. The vertical coordinate is the normalized frequency, σ/f. For the E grid, the results are meaningful only in the triangular region for which $kd^* + ld^* \le 2\pi$. The left column shows results for $\lambda/d = 2$, and the right column for $\lambda/d = 0.1$.

Now consider an unstaggered grid for the integration of (7.31) - (7.33), which was called the Z grid by Randall (1994). This grid is also illustrated in Fig. 7.2. Inspection shows that with the Z grid the components of the divergent part of the wind "want" to be staggered as in the C grid, while the components of the rotational part of the wind "want" to be staggered as in the D grid. This means that the Z grid does not correspond to any of the grids A through E.

No averaging is required with the Z grid. The only spatial differential operator appearing in (7.31) - (7.33) is the Laplacian, $\nabla^2(\ )$, which is applied to h in the divergence equation. With the usual centered finite-difference stencils, the finite-difference approximation to $\nabla^2 h$ is defined at the same point as h itself. An unstaggered grid is thus a natural choice for the numerical integration of (7.31) - (7.33).

Fig. 7.3 shows that the dispersion relation for the Z grid is very close to that of the C grid, for $\lambda/d = 2$, but is drastically different for $\lambda/d = 0.1$. Whereas the C grid behaves very badly for $\lambda/d = 0.1$, the dispersion relation obtained with the Z grid is qualitatively insensitive to the value of λ/d; it resembles the dispersion relation for the continuous equations, in that the phase speed increases monotonically with wave number and the group speed is non-zero for all wave numbers. Since the Z grid is unstaggered, collapsing it to one dimension has no effect.

The discussion presented above suggests that geostrophic adjustment in shallow water is well simulated on an unstaggered grid when the vorticity and divergence equations are used. The vorticity and divergence equations are routinely used in global spectral models, but are rarely used in global finite-difference models. The reason seems to be that it is necessary to solve elliptic equations to obtain the winds from the vorticity and divergence, e.g., to evaluate the advection terms of the nonlinear primitive equations. As discussed later, such solution procedures can be computationally expensive in finite-difference models, but are not expensive in spectral models. It may be appropriate to re-examine this point in the light of modern algorithms for solving linear systems, e.g., multi-grid methods.

7.5 Time-differencing schemes for the shallow-water equations

In this section, we illustrate properties of various time differencing schemes applied to the one-dimensional shallow water equations with rotation, linearized about a mean zonal flow that is assumed to be in geostrophic balance. The equations are

$$\begin{aligned} \frac{\partial u}{\partial t} + U\frac{\partial u}{\partial x} &= fv - g\frac{\partial h}{\partial x}\,, \\ \frac{\partial v}{\partial t} + U\frac{\partial v}{\partial x} &= -fu\,, \\ \frac{\partial h}{\partial t} + U\frac{\partial h}{\partial x} - \frac{fU}{g}v &= -H\frac{\partial u}{\partial x}\,. \end{aligned} \tag{7.35}$$

Here we have used the assumed geostrophy of the mean zonal flow to write $\frac{dH}{dy} = -\frac{fU}{g}$. Geostrophic balance is obtained by neglecting the terms on the left-hand sides of (7.35). For

$U = 0$, the solutions correspond to dispersive inertia-gravity waves and stationary geostrophic motion.

We first examine the exact solution of (7.35). Assume that $(u, v, h) \propto e^{ik(x-ct)}$. This leads to

$$\begin{aligned} (U-c)u + i\frac{f}{k}v + gh &= 0 \ , \\ -i\frac{f}{k}u + (U-c)v &= 0 \ , \\ Hu + i\frac{fU}{kg}v + (U-c)h &= 0 \ . \end{aligned} \tag{7.36}$$

To have a non-trivial solution, c must satisfy

$$(c-U)^3 - \left(gH + \frac{f^2}{k^2}\right)(c-U) - \frac{f^2}{k^2}U = 0 \ . \tag{7.37}$$

Obviously there are three solutions. Assume that $\left(gH + \frac{f^2}{k^2}\right) \gg U^2$, which means that the gravity-wave phase speed is much faster than U. If $c - U \sim O\left[\left(gH + \frac{f^2}{k^2}\right)^{\frac{1}{2}}\right]$, then $c - U$ is approximately given by the balance of the first two terms in (7.37). In that case,

$$c \cong c_{GI} \equiv U \pm \left(gH + \frac{f^2}{k^2}\right)^{\frac{1}{2}} \text{ (gravity-inertia wave).} \tag{7.38}$$

If $c - U \sim O(U)$, $c - U$ is approximately given by the balance of the last two terms. Then

$$c \cong c_{QG} \equiv \left(\frac{gH}{gH + \frac{f^2}{k^2}}\right) U \text{ (quasi-geostrophic wave).} \tag{7.39}$$

Now we carry out the corresponding analysis for the finite-difference system. Suppose that we adopt a staggered grid as shown in Fig. 7.4. This is one-dimensional version

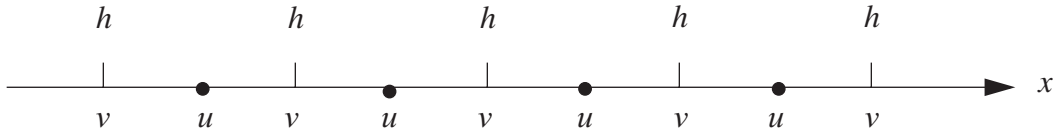

Figure 7.4: A one-dimensional version of the C grid.

of the C-grid.With second-order centered space differencing, we obtain

$$\frac{du}{dt}_{j+\frac{1}{2}} + U\left(\frac{u_{j+\frac{3}{2}} - u_{j-\frac{1}{2}}}{2\Delta x}\right) = f\left(\frac{v_j + v_{j+1}}{2}\right) - g\left(\frac{h_{j+1} - h_j}{\Delta x}\right) ,$$

$$\frac{dv_j}{dt} + U\left(\frac{v_{j+1} - v_{j-1}}{2\Delta x}\right) = -f\left(\frac{u_{j+\frac{1}{2}} + u_{j-\frac{1}{2}}}{2}\right) , \tag{7.40}$$

$$\frac{dh_j}{dt} + U\left(\frac{h_{j+1} - h_{j-1}}{2\Delta x}\right) - \frac{fU}{g}v_j = -H\left(\frac{u_{j+\frac{1}{2}} - u_{j-\frac{1}{2}}}{\Delta x}\right) .$$

Assuming solutions of the form $(u, v, h) = Re[(\hat{u}, \hat{v}, \hat{h})e^{jk\Delta x}]$, we obtain

$$\frac{d\hat{u}}{dt} + U\hat{u}\left(\frac{e^{ik\Delta x} - e^{-ik\Delta x}}{2\Delta x}\right) = f\hat{v}\left(\frac{e^{i\frac{1}{2}k\Delta x} + e^{-i\frac{1}{2}k\Delta x}}{2}\right) - g\hat{h}\left(\frac{e^{i\frac{1}{2}k\Delta x} - e^{-i\frac{1}{2}k\Delta x}}{\Delta x}\right) ,$$

$$\frac{d\hat{v}}{dt} + U\hat{v}\left(\frac{e^{ik\Delta x} - e^{-ik\Delta x}}{2\Delta x}\right) = -f\hat{u}\left(\frac{e^{i\frac{1}{2}k\Delta x} + e^{-i\frac{1}{2}k\Delta x}}{2}\right) , \tag{7.41}$$

$$\frac{d\hat{h}}{dt} + U\hat{h}\left(\frac{e^{ik\Delta x} - e^{-ik\Delta x}}{2\Delta x}\right) - \frac{fU}{g}\hat{v} = -H\hat{u}\left(\frac{e^{i\frac{1}{2}k\Delta x} - e^{-i\frac{1}{2}k\Delta x}}{\Delta x}\right) ,$$

which reduces to

$$\frac{d\hat{u}}{dt} + U\left(\frac{\sin k\Delta x}{k\Delta x}\right)\hat{u}ik = f\hat{v}\cos\frac{k\Delta x}{2} - g\hat{h}ik\left(\frac{\sin\frac{k\Delta x}{2}}{\frac{k\Delta x}{2}}\right),$$

$$\frac{d\hat{v}}{dt} + U\left(\frac{\sin k\Delta x}{k\Delta x}\right)\hat{v}ik = -f\hat{u}\cos\frac{k\Delta x}{2}, \tag{7.42}$$

$$\frac{d\hat{h}}{dt} + U\left(\frac{\sin k\Delta x}{k\Delta x}\right)ki\hat{h} - \frac{fU}{g}\hat{v} = -H\hat{u}ik\left(\frac{\sin\frac{k\Delta x}{2}}{\frac{k\Delta x}{2}}\right),$$

or, finally,

$$\frac{d\hat{u}}{dt} + U^* ik\hat{u} = f^*\hat{v} - g^* ik\hat{h},$$

$$\frac{d\hat{v}}{dt} + U^* ik\hat{v} = -f^*\hat{u}, \tag{7.43}$$

$$\frac{d\hat{h}}{dt} + U^* ik\hat{h} - \frac{fU}{g}\hat{v} = -H^* ik\hat{u},$$

where, for convenience, we define

$$U^* \equiv \left(\frac{\sin k\Delta x}{k\Delta x}\right)U,\ g^* \equiv \left(\frac{\sin\frac{k\Delta x}{2}}{\frac{k\Delta x}{2}}\right)g,\ H^* \equiv \left(\frac{\sin\frac{k\Delta x}{2}}{\frac{k\Delta x}{2}}\right)H, \text{ and } f^* \equiv \left(\cos\frac{k\Delta x}{2}\right)f. \tag{7.44}$$

We can write (7.43) as

$$\frac{d}{dt}\begin{bmatrix}\hat{u}\\ \hat{v}\\ \hat{h}\end{bmatrix} = -ik\begin{bmatrix}U^* & i\frac{f^*}{k} & g^*\\ -i\frac{f^*}{k} & U^* & 0\\ H^* & i\frac{fU}{kg} & U^*\end{bmatrix}\begin{bmatrix}\hat{u}\\ \hat{v}\\ \hat{h}\end{bmatrix} \tag{7.45}$$

Now assume time-dependence of the form e^{-ikc^*t}, so that (7.49) becomes

$$-ikc^*\begin{bmatrix}\hat{u}\\ \hat{v}\\ \hat{h}\end{bmatrix} = -ik\begin{bmatrix}U^* & i\frac{f^*}{k} & g^*\\ -i\frac{f^*}{k} & U^* & 0\\ H^* & i\frac{fU}{kg} & U^*\end{bmatrix}\begin{bmatrix}\hat{u}\\ \hat{v}\\ \hat{h}\end{bmatrix} \tag{7.46}$$

or

$$\begin{bmatrix}U^*-c^* & i\frac{f^*}{k} & g^*\\ -i\frac{f^*}{k} & U^*-c^* & 0\\ H^* & i\frac{fU}{kg} & U^*-c^*\end{bmatrix}\begin{bmatrix}\hat{u}\\ \hat{v}\\ \hat{h}\end{bmatrix} = 0 \tag{7.47}$$

For nontrivial solutions, we must require that

$$Det\begin{bmatrix}U^*-c^* & i\frac{f^*}{k} & g^*\\ -i\frac{f^*}{k} & U^*-c^* & 0\\ H^* & i\frac{fU}{kg} & U^*-c^*\end{bmatrix} = 0\,, \tag{7.48}$$

which leads to

$$(c^* - U^*)^3 - \left(\frac{f^{*2}}{k^2} + g^* H^*\right)(c^* - U^*) - \left(\frac{g^*}{g}\right)\left(\frac{f^* f}{k^2}\right) U = 0 \tag{7.49}$$

Compare (7.49) with (7.37). As in the differential case, the approximate solutions are

$$c^*_{GI} \cong U^* \pm \left(g^* H^* + \frac{f^{*2}}{k^2}\right)^{\frac{1}{2}} \text{ (gravity-inertia waves),} \tag{7.50}$$

$$c^*_{QG} \cong \frac{\left(\frac{f^{*2}}{k^2} + g^* H^*\right) U^* - \left(\frac{g^*}{g}\right)\left(\frac{f^* f}{k^2}\right) U}{\frac{f^{*2}}{k^2} + g^* H^*} \text{ (quasi-geostrophic waves).} \tag{7.51}$$

You should be able to show that $c^*_{QG} = 0$ for wave length $2\Delta x$.

The preceding discussion follows our usual approach: Analyze a simplified version of the continuous problem first, and derive some key results, e.g., the dispersion equation for linear waves. Then do the corresponding analysis for the finite-difference system, and compare the finite-difference results with the continuous results. S.

Von Neumann's method, applied to a hyperbolic system of equations, tests the stability of each mode. For most time-differencing schemes, the amplification factor depends on $\Omega \equiv c^* k \Delta t$; note that the computational phase speed appears here. When we apply a scheme for which $|\Omega| \le 1$ is required for stability, we must satisfy

$$|\Omega_{GI}| \equiv \left|c^*_{GI}\right| k\Delta t \le 1 \tag{7.52}$$

for all k. If we satisfy (7.52), we will automatically satisfy

$$|\Omega_{QG}| \equiv \left|c^*_{QG}\right| k\Delta t \ll 1 \,, \tag{7.53}$$

because $\left|c^*_{QG}\right| \ll \left|c^*_{GI}\right|$. In other words, the gravity-inertia waves determine the allowed time step.

From (7.50), we obtain

$$|\Omega_{GI}| \le k\left[|U^*| + \left(g^*H^* + \frac{f^{*2}}{k^2}\right)^{\frac{1}{2}}\right]\Delta t$$

$$= \left\{\frac{\sin k\Delta x}{\Delta x}|U| + \left[\left(\frac{\sin\frac{k\Delta x}{2}}{\frac{\Delta x}{2}}\right)^2 gH + f^2\left(\cos\frac{k\Delta x}{2}\right)^2\right]^{\frac{1}{2}}\right\}\Delta t$$

$$\le \left\{|U| + [4gH + f^2(\Delta x)^2]^{\frac{1}{2}}\right\}\frac{\Delta t}{\Delta x}\,. \tag{7.54}$$

When $|U| \ll \sqrt{gH}$ (wind speed is slow compared to gravity-wave phase speed) and $f^2(\Delta x)^2 \ll 4gH$ (grid size is small compared to the radius of deformation), the stability criterion becomes, approximately,

$$2\sqrt{gH}\frac{\Delta t}{\Delta x} < 1\,. \tag{7.55}$$

7.6 Conservation of mass, kinetic energy, and potential energy in one-dimensional divergent flow

Consider shallow water in one dimension, without rotation, and with bottom topography. The prognostic variables are the water depth or mass, h, and the speed, u. The exact equations are

$$\frac{\partial h}{\partial t} + \frac{\partial}{\partial x}(hu) = 0\,, \tag{7.56}$$

and

$$\frac{\partial u}{\partial t} + \frac{\partial}{\partial x}[K + g(h + h_S)] = 0\,. \tag{7.57}$$

Here $K \equiv \frac{1}{2}u^2$ is the kinetic energy per unit mass, g is the acceleration of gravity, and h_S is the height of the "topography." Note that in (7.57) the vorticity has been assumed to vanish,

which is reasonable in the absence of rotation and in one dimension.

The flux form of the kinetic energy equation can be derived by multiplying (7.56) by K and (7.57) by hu, and adding the results, to obtain

$$\frac{\partial}{\partial t}(hK) + \frac{\partial}{\partial x}(huK) + hu\frac{\partial}{\partial x}[g(h + h_S)] = 0 . \tag{7.58}$$

The last term of (7.58) represents conversion between potential and kinetic energy.

The potential energy equation can be derived by multiplying (7.56) by $g(h + h_S)$ to obtain

$$\frac{\partial}{\partial t}\left[hg\left(h_S + \frac{1}{2}h\right)\right] + g(h + h_S)\frac{\partial}{\partial x}(hu) = 0 , \tag{7.59}$$

or

$$\frac{\partial}{\partial t}\left[hg\left(h_S + \frac{1}{2}h\right)\right] + \frac{\partial}{\partial x}[hug(h + h_S)] - hu\frac{\partial}{\partial x}[g(h + h_S)] = 0 \tag{7.60}$$

The last term of (7.60) represents conversion between kinetic and potential energy; compare with (7.58). In deriving (7.59), we have assumed that h_S is independent of time.

When we add (7.58) and (7.59) the energy conversion terms cancel, and we obtain a statement of the conservation of total energy, i.e.

$$\frac{\partial}{\partial t}\left\{h\left[K + g\left(h_S + \frac{1}{2}h\right)\right]\right\} + \frac{\partial}{\partial x}\{hu[K + g(h + h_S)]\} = 0 . \tag{7.61}$$

Now consider finite-difference approximations to (7.56) and (7.57). We keep the time derivatives continuous, and explore the effects of space differencing only. We use a staggered grid, with *h* defined at integer points (hereafter called mass points) and *u* at half-integer points (hereafter called wind points). The grid spacing, Δx, is assumed to be uniform. The grid is shown in Fig. 7.5. It can be viewed as a one-dimensional version of the C grid. The finite

Figure 7.5: The staggered grid used in the one-dimensional case.

difference version of the mass conservation equation is

$$\frac{d}{dt}h_i + \frac{1}{\Delta x}\left[(hu)_{i+\frac{1}{2}} - (hu)_{i-\frac{1}{2}}\right] = 0\,. \tag{7.62}$$

The mass fluxes, $(hu)_{i+\frac{1}{2}}$ and $(hu)_{i-\frac{1}{2}}$, are undefined at this stage, except that they are subscripted so as to indicate that they reside at wind points. The finite difference version of the momentum equation is

$$\frac{d}{dt}u_{i+\frac{1}{2}} + \left(\frac{K_{i+1} - K_i}{\Delta x}\right) + g\left[\frac{(h+h_S)_{i+1} - (h+h_S)_i}{\Delta x}\right] = 0\,. \tag{7.63}$$

The kinetic energy per unit mass, K_i, is undefined at this stage, but resides at mass points.

The finite-difference approximations used in (7.62) and (7.63) are consistent with second-order accuracy in space, although we cannot really determine the order of accuracy until the finite-difference forms of the mass flux and kinetic energy are specified.

Multiply (7.63) by $(hu)_{i+\frac{1}{2}}$ to obtain

$$(hu)_{i+\frac{1}{2}}\frac{d}{dt}u_{i+\frac{1}{2}} + (hu)_{i+\frac{1}{2}}\left(\frac{K_{i+1} - K_i}{\Delta x}\right) + g(hu)_{i+\frac{1}{2}}\left[\frac{(h+h_S)_{i+1} - (h+h_S)_i}{\Delta x}\right] = 0 \tag{7.64}$$

.

Rewrite (7.64) for grid point $i - \frac{1}{2}$, simply by subtracting one from each subscript:

$$(hu)_{i-\frac{1}{2}}\frac{d}{dt}u_{i-\frac{1}{2}} + (hu)_{i-\frac{1}{2}}\left(\frac{K_i - K_{i-1}}{\Delta x}\right) + g(hu)_{i-\frac{1}{2}}\left[\frac{(h+h_S)_i - (h+h_S)_{i-1}}{\Delta x}\right] = 0\,. \tag{7.65}$$

Now add (7.64) and (7.65), and multiply the result by $\frac{1}{2}$:

$$\frac{1}{2}\left[(hu)_{i+\frac{1}{2}}\frac{d}{dt}u_{i+\frac{1}{2}}+(hu)_{i-\frac{1}{2}}\frac{\partial}{\partial t}u_{i-\frac{1}{2}}\right]$$

$$+\frac{1}{2}\left[(hu)_{i+\frac{1}{2}}\left(\frac{K_{i+1}-K_i}{\Delta x}\right)+(hu)_{i-\frac{1}{2}}\left(\frac{K_i-K_{i-1}}{\Delta x}\right)\right]$$

$$+\frac{g}{2}\left\{(hu)_{i+\frac{1}{2}}\left[\frac{(h+h_S)_{i+1}-(h+h_S)_i}{\Delta x}\right]+(hu)_{i-\frac{1}{2}}\left[\frac{(h+h_S)_i-(h+h_S)_{i-1}}{\Delta x}\right]\right\}=0\ . \tag{7.66}$$

This is an advective form of the kinetic energy equation.

Now we try to derive, from (7.66) and (7.62), a flux form of the kinetic energy equation. Multiply (7.62) by K_i:

$$K_i\left\{\frac{dh_i}{dt}+\left[\frac{(hu)_{i+\frac{1}{2}}-(hu)_{i-\frac{1}{2}}}{\Delta x}\right]\right\}=0\,. \tag{7.67}$$

Keep in mind that we still do not know what K_i is; we have just multiplied the continuity equation by a mystery variable. Add (7.67) and (7.66) to obtain

$$K_i\frac{dh_i}{dt}+\frac{1}{2}\left[(hu)_{i+\frac{1}{2}}\frac{d}{dt}u_{i+\frac{1}{2}}+(hu)_{i-\frac{1}{2}}\frac{d}{dt}u_{i-\frac{1}{2}}\right]$$

$$+\left\{(hu)_{i+\frac{1}{2}}\left[\frac{K_i}{\Delta x}+\frac{1}{2}\left(\frac{K_{i+1}-K_i}{\Delta x}\right)\right]-(hu)_{i-\frac{1}{2}}\left[\frac{K_i}{\Delta x}-\frac{1}{2}\left(\frac{K_i-K_{i-1}}{\Delta x}\right)\right]\right\}$$

$$+g\left\{(hu)_{i+\frac{1}{2}}\frac{[(h+h_S)_{i+1}-(h+h_S)_i]}{2\Delta x}+(hu)_{i-\frac{1}{2}}\frac{[(h+h_S)_i-(h+h_S)_{i-1}]}{2\Delta x}\right\}=0\ . \tag{7.68}$$

Eq. (7.68) "should" be a flux form of the kinetic energy equation. As demonstrated below, we can ensure that it is by adopting suitable definitions of the mass fluxes and the kinetic energy.

The advection terms on the second line of (7.68) are very easy to deal with. They can be rearranged to

$$\frac{1}{\Delta x}\left[(hu)_{i+\frac{1}{2}}\frac{1}{2}(K_{i+1}+K_i)-(hu)_{i-\frac{1}{2}}\frac{1}{2}(K_i+K_{i-1})\right]. \tag{7.69}$$

This has the form of a "finite-difference flux divergence." The conclusion is that these terms are consistent with kinetic energy conservation simply by virtue of their form, regardless of the definitions that we adopt for the mass flux and the kinetic energy.

Next, consider the energy conversion terms on the last line of (7.68), i.e.

$$g\left\{(hu)_{i+\frac{1}{2}}\left[\frac{(h+h_S)_{i+1}-(h+h_S)_i}{2\Delta x}\right]+(hu)_{i-\frac{1}{2}}\left[\frac{(h+h_S)_i-(h+h_S)_{i-1}}{2\Delta x}\right]\right\}. \tag{7.70}$$

The finite-difference form of the potential energy equation can be derived by multiplying (7.62) by $g(h+h_S)_i$:

$$\frac{\partial}{\partial t}\left[h_i g\left(h_S+\frac{1}{2}h\right)_i\right]+g(h+h_S)_i\left[\frac{(hu)_{i+\frac{1}{2}}-(hu)_{i-\frac{1}{2}}}{\Delta x}\right]=0. \tag{7.71}$$

This is analogous to (7.59). We want to recast (7.71) so that we see advection of potential energy, as well as the energy conversion term corresponding to (7.70); compare with (7.60). We write

$$\begin{gathered}\frac{\partial}{\partial t}\left[h_i g\left(h_S+\frac{1}{2}h\right)_i\right]+ADV_i\\ -\frac{g}{2}\left\{(hu)_{i+\frac{1}{2}}\left[\frac{(h+h_S)_{i+1}-(h+h_S)_i}{\Delta x}\right]+(hu)_{i-\frac{1}{2}}\left[\frac{(h+h_S)_i-(h+h_S)_{i-1}}{\Delta x}\right]\right\}=0,\end{gathered} \tag{7.72}$$

where "ADV_i" represents the advection of potential energy, in flux form. We require that (7.72) be consistent with (7.71), and ask what form of ADV_i is implied by this requirement. In this way, we obtain

$$\begin{aligned}ADV_i = {} & (hu)_{i+\frac{1}{2}}\left\{\frac{g}{2\Delta x}[(h+h_S)_{i+1}+(h+h_S)_i]\right\}\\ & -(hu)_{i-\frac{1}{2}}\left\{\frac{g}{2\Delta x}[(h+h_S)_i+(h+h_S)_{i-1}]\right\}.\end{aligned} \tag{7.73}$$

Because (7.73) has the form of a finite-difference flux divergence, total energy will be conserved, regardless of the definition that we adopt for the finite-difference mass flux.

Finally, consider the time-rate-of-change terms of (7.68). Obviously, the first line of (7.68) should be interpreted as $\frac{\partial}{\partial t}(K_i h_i)$, i.e.

$$\frac{d}{dt}(K_i h_i) = K_i \frac{\partial h_i}{\partial t} + \frac{1}{2}\left[(hu)_{i+\frac{1}{2}} \frac{\partial}{\partial t} u_{i+\frac{1}{2}} + (hu)_{i-\frac{1}{2}} \frac{\partial}{\partial t} u_{i-\frac{1}{2}} \right], \tag{7.74}$$

from which it follows that

$$h_i \frac{d}{dt} K_i = \frac{1}{2}\left[(hu)_{i+\frac{1}{2}} \frac{\partial}{\partial t} u_{i+\frac{1}{2}} + (hu)_{i-\frac{1}{2}} \frac{\partial}{\partial t} u_{i-\frac{1}{2}} \right]. \tag{7.75}$$

At this point it is convenient to introduce an interpolated mass variable located at the wind points. This is defined by

$$\hat{h}_{i+\frac{1}{2}} u_{i+\frac{1}{2}} \equiv (hu)_{i+\frac{1}{2}} . \tag{7.76}$$

This is not an assumption. We have merely traded one undefined symbol, namely $(hu)_{i+\frac{1}{2}}$, for another one, namely $\hat{h}_{i+\frac{1}{2}}$. By substituting (7.76) into (7.75), we obtain

$$h_i \frac{\partial}{\partial t} K_i = \frac{1}{4}\left(\hat{h}_{i+\frac{1}{2}} \frac{\partial}{\partial t} u^2_{i+\frac{1}{2}} + \hat{h}_{i-\frac{1}{2}} \frac{\partial}{\partial t} u^2_{i-\frac{1}{2}} \right) . \tag{7.77}$$

This is a requirement, although as we shall see below it is not really quite as strict as it appears. Inspection of (7.77) shows that our requirement involves the two undefined symbols K_i and $\hat{h}_{i+\frac{1}{2}}$. We can satisfy the requirement by choosing proper definitions for these symbols. There are at least two different ways to do this.

The first possibility is to define the kinetic energy per unit mass by

$$K_i \equiv \frac{1}{4}\left(u^2_{i+\frac{1}{2}} + u^2_{i-\frac{1}{2}} \right) . \tag{7.78}$$

Substitution into (7.77) gives

$$h_i \left(\frac{\partial}{\partial t} u^2_{i+\frac{1}{2}} + \frac{\partial}{\partial t} u^2_{i-\frac{1}{2}} \right) = \hat{h}_{i+\frac{1}{2}} \frac{\partial}{\partial t} u^2_{i+\frac{1}{2}} + \hat{h}_{i-\frac{1}{2}} \frac{\partial}{\partial t} u^2_{i-\frac{1}{2}} . \tag{7.79}$$

We cannot simply set $\hat{h}_{i+\frac{1}{2}} = h_i$ and $\hat{h}_{i-\frac{1}{2}} = h_i$, because taken together these amount to a contradiction; the first says that "the interpolated mass at a wind point is equal to the predicted mass to the left," while the second says that "the interpolated mass at a wind point is equal to the predicted mass to the right." These statements cannot both be true except in the trivial case of constant h.

As an alternative, we can define the interpolated mass to be the arithmetic mean of the two neighboring predicted masses:

$$\hat{h}_{i+\frac{1}{2}} = \frac{1}{2}(h_i + h_{i+1}) . \tag{7.80}$$

Substitution into (7.79) gives

$$h_i\left(\frac{\partial}{\partial t}u^2_{i+\frac{1}{2}} + \frac{\partial}{\partial t}u^2_{i-\frac{1}{2}}\right) = \frac{1}{2}(h_i + h_{i+1})\frac{\partial}{\partial t}u^2_{i+\frac{1}{2}} + \frac{1}{2}(h_{i-1} + h_i)\frac{\partial}{\partial t}u^2_{i-\frac{1}{2}} \quad , \tag{7.81}$$

and this can be rearranged to

$$h_i\left(\frac{\partial}{\partial t}u^2_{i+\frac{1}{2}} + \frac{\partial}{\partial t}u^2_{i-\frac{1}{2}}\right) = h_{i+1}\frac{\partial}{\partial t}u^2_{i+\frac{1}{2}} + h_{i-1}\frac{\partial}{\partial t}u^2_{i-\frac{1}{2}} \quad . \tag{7.82}$$

Now it appears that we are really in trouble, since (7.82) cannot be satisfied unless h is uniform on the grid. We are rescued, however, by the fact that (7.82) does not really have to be satisfied to allow kinetic energy conservation. All we really need to require is that when (7.82) is summed over the entire grid, the sum of the left side is equal to the sum of the right side. This will be the case, since the first term on the left will cancel, in the sum over grid points, with the second term on the right, and vice versa.

Note that although the preceding discussion deals with the time-rate-of-change terms of (7.68), the issues have nothing to do with time differencing; we have been discussing space differencing only.

A second way to define the kinetic energy is:

$$h_i K_i \equiv \frac{1}{4}\left(\hat{h}_{i+\frac{1}{2}}u^2_{i+\frac{1}{2}} + \hat{h}_{i-\frac{1}{2}}u^2_{i-\frac{1}{2}}\right) \quad . \tag{7.83}$$

Here we have used a mass weighting, and we revert to a "general" form of the wind-point masses. Substitution of (7.83) into the left-hand side of (7.74) gives

$$\frac{1}{4}\frac{\partial}{\partial t}\left(\hat{h}_{i+\frac{1}{2}}u^2_{i+\frac{1}{2}} + \hat{h}_{i-\frac{1}{2}}u^2_{i-\frac{1}{2}}\right) = K_i\frac{\partial h_i}{\partial t} + \frac{1}{4}\left(\hat{h}_{i+\frac{1}{2}}\frac{\partial}{\partial t}u^2_{i+\frac{1}{2}} + \hat{h}_{i-\frac{1}{2}}\frac{\partial}{\partial t}u^2_{i-\frac{1}{2}}\right) \quad , \tag{7.84}$$

which can be simplified to

$$\frac{1}{4}u^2_{i+\frac{1}{2}}\frac{\partial}{\partial t}\hat{h}_{i+\frac{1}{2}} + \frac{1}{4}u^2_{i-\frac{1}{2}}\frac{\partial}{\partial t}\hat{h}_{i-\frac{1}{2}} = K_i\frac{\partial h_i}{\partial t} \quad . \tag{7.85}$$

Multiply both sides of (7.85) by h_i and use (7.83) again to obtain

$$h_i\left(u^2_{i+\frac{1}{2}}\frac{\partial}{\partial t}\hat{h}_{i+\frac{1}{2}} + u^2_{i-\frac{1}{2}}\frac{\partial}{\partial t}\hat{h}_{i-\frac{1}{2}}\right) = \left(\hat{h}_{i+\frac{1}{2}}u^2_{i+\frac{1}{2}} + \hat{h}_{i-\frac{1}{2}}u^2_{i-\frac{1}{2}}\right)\frac{\partial h_i}{\partial t} \quad . \tag{7.86}$$

If we use (7.80) again, we obtain

$$\begin{aligned} &h_i u^2_{i+\frac{1}{2}}\left(\frac{\partial h_i}{\partial t} + \frac{\partial h_{i+1}}{\partial t}\right) + h_i u^2_{i-\frac{1}{2}}\left(\frac{\partial h_i}{\partial t} + \frac{\partial h_{i-1}}{\partial t}\right) \\ &= \left[(h_{i+1} + h_i)u^2_{i+\frac{1}{2}} + (h_i + h_{i-1})u^2_{i-\frac{1}{2}}\right]\frac{\partial h_i}{\partial t}, \end{aligned} \tag{7.87}$$

or

$$h_i u^2_{i+\frac{1}{2}}\frac{\partial h_{i+1}}{\partial t} + h_i u^2_{i-\frac{1}{2}}\frac{\partial h_{i-1}}{\partial t} = h_{i+1}u^2_{i+\frac{1}{2}}\frac{\partial h_i}{\partial t} + h_{i-1}u^2_{i-\frac{1}{2}}\frac{\partial h_i}{\partial t} \quad . \tag{7.88}$$

This, of course, is not true. When summed over the whole domain, though, the first term on the left-hand side of (7.88) cancels with the second term on the right-hand side, and vice versa. The conclusion is that, for the domain as a whole, kinetic energy is again conserved. In fact, the sum over the domain of $h_i K_i$ given by (7.78) is equal to the sum over the domain of $h_i K_i$ given by (7.83).

In summary, we have explored the conservation properties of spatial finite-difference approximations of the momentum and continuity equations for one-dimensional non-rotating flow, using a staggered grid with second-order space differencing. By choosing particular forms for the kinetic energy per unit mass and the interpolated masses at wind points, we can guarantee conservation of kinetic energy under advection, conservation of potential energy under advection, and conservation of total energy under the influence of the energy conversion terms, as well as conservation of mass.

7.7 Summary

With the one-dimensional advection equation we had "propagation" in one direction only, and with a second-order space-centered scheme for this equation we had to contend with one physical mode and one computational mode. The one-dimensional wave equation is equivalent to a pair of one-dimensional advection equations, so that we have a pair of physical modes and a pair of computational modes -- one of each propagating in each of the two spatial directions.

The advection equation "prefers" uncentered space differencing, but centered space differencing is most natural with the wave equation.

An unstaggered grid permits computational modes in space, essentially allowing two distinct solutions that live separate lives and do not interact. A staggered grid helps to overcome the problem of computational modes in space. Many staggering schemes are possible, especially in two or three dimensions. Some of the schemes give particularly realistic propagation characteristics, allowing realistic simulation of such important processes as geostrophic adjustment.

In a model that permits both quasi-geostrophic motions and inertia-gravity waves, such as a primitive-equation model, the time step is normally limited by the stability criterion for the inertia-gravity waves.

Finite-difference systems can be constructed so as to conserve the sum of potential and kinetic energy in a divergent flow.

Problems

1. Repeat the analysis of Section 7.5 using the Z grid instead of the C grid.

2. Consider the linearized (about a resting basic state) shallow-water equations without rotation on the one-dimensional versions of the A grid and the C grid. Let the distance between neighboring mass points be d on both grids. Use leapfrog time differencing. Derive the stability criteria for both cases, and compare the two results.

3. Write down differential-difference equations for the linearized (about a resting basic state) one-dimensional shallow water equations without rotation on an *unstaggered* grid (the A grid), and using fourth-order accuracy for the spatial derivatives. (It is not necessary to prove the order of accuracy in this problem.) Perform an analysis to determine whether or not the scheme has computational modes. Compare with the corresponding second-order scheme.

4. Program the two-dimensional linearized shallow water equations for the A-grid and the C-grid, using a mesh of 101 x 101 mass points, with periodic boundary conditions in both directions. Use leapfrog time differencing. Set $g = 0.1$ m s^{-2}, $H = 10^3$ m, $f = 0.5$ x 10^{-4} s^{-1}, and $d = 10^5$ m.

   In the square region

$$\begin{aligned} 45 \le i \le 55 \ , \\ 45 \le j \le 55 \ , \end{aligned} \tag{7.89}$$

   apply a forcing in the continuity equation, of the form

$$\left(\frac{\partial h}{\partial t}\right)_{\text{noise}} = (-1)^{i+j} N e^{i\omega_N t} \ , \tag{7.90}$$

   and set $\left(\frac{\partial h}{\partial t}\right)_{\text{noise}} = 0$ at all other grid points. Adopt the values $\omega_N = 2\pi \times 10^{-3}$ s^{-1}; and $N = 10^{-4}$ m s^{-1}. In addition, for the entire domain apply a forcing of the form

$$\left(\frac{\partial h}{\partial t}\right)_{\text{smooth}} = S \sin\left(\frac{2\pi x}{L}\right) \sin\left(\frac{2\pi y}{L}\right) e^{i\omega_S t} \tag{7.91}$$

with $\omega_s = \frac{2\pi\sqrt{gH}}{L}$ s^{-1} and $S = 10^{-4}$ m s^{-1}. Here L is 101 x d, the width of the domain.

Finally, include damping in the momentum equations, of the form

$$\left(\frac{\partial u}{\partial t}\right)_{\text{fric}} = -Ku \ , \qquad \left(\frac{\partial v}{\partial t}\right)_{\text{fric}} = -Kv \ , \tag{7.92}$$

where $K = 2 \times 10^{-5} s^{-1}$. Because the model has both forcing and damping, it is possible to obtain a statistically steady solution.

a) Analyze the stability of the two models without the forcing or damping terms. Using your results, choose a suitable time step for each model. Note: The forcing and damping terms are not expected to limit the time step, so we simply omit them in our analysis of the stability criterion.

b) As initial conditions, put $u = 0$, $v = 0$, and $h = 0$. Run both versions of the model for at least 10^5 simulated seconds, and analyze the results. Your analysis should compare various aspects of the solutions, in light of the discussion given in this chapter.

c) Repeat your runs using $f = 2 \times 10^{-4} s^{-1}$. Discuss the changes in your results.